[11] S. C. Frautschi and J. D. Walecka, Phys. Rev. 120, 1486 (1960).
[12] G. F. Chew and F. E. Low, Phys. Rev. 101, 1570 (1956).
[13] V. Singh and B. M. Udgaonkar, Phys. Rev. 130, 1177 (1963).
[14] V. Singh and B. M. Udgaonkar, Phys. Rev. 128, 1820 (1962).
[15] V. F. Šachl, Phys. Rev. D 3, 2065 (1971). In this paper the specified calculations of the present approach regarding one point s of the P_{13} amplitude at threshold $s=s_{\text{thr}}$, i.e., the scattering length a_{13}, were published. There are three misprints to be corrected: The factor m^2 in formula (6) of Ref. 15 should be m^3. The minus sign is omitted in Eq. (13). The factor $\frac{1}{18}$ in Eq. (14) should be $\frac{8}{9}$. For the correct forms see also Eqs. (9), (16), and (17) of the present paper.
[16] S. W. Barnes *et al.*, Phys. Rev. 117, 116 (1960); 117, 238 (1960).
[17] In that case also the subtraction constant is fixed uniquely and depends on the CDD parameters. See, e.g., G. R. Bart and R. L. Warnock, Phys. Rev. D 3, 1429 (1971).

PHYSICAL REVIEW D VOLUME 5, NUMBER 7 1 APRIL 1972

Eikonal Regge Model for the Processes $\pi^{\pm}p\to A_1^{\pm}p$ at Small Momentum Transfers

K. Ahmed
Institute of Physics, University of Islamabad, Rawalpindi, Pakistan

and

M. B. Bari
Institute of Physics, High Energy Group, Tabriz University, Tabriz, Iran

and

V. P. Seth
International Centre for Theoretical Physics, Trieste, Italy
(Received 30 September 1971)

An eikonal Regge representation is set up for the helicity amplitudes in the process $\pi p \to A_1 p$. These amplitudes are then used to calculate the density-matrix elements of $A_1(1^+)$, which are in agreement with the data.

I. INTRODUCTION

The power of the eikonal or absorption model of generating the Regge-cut effects has been used extensively with considerable success in the elastic[1] and also inelastic[2] scatterings. These cuts are found to satisfy properties very similar to those one expects from the study of Feynman graphs.[3] Phenomenologically, a definite evidence for the existence of the Regge cuts, in our opinion, lies not so much in their fitting the data on cross sections as in their giving the correct predictions on measurements like polarizations, density-matrix elements, etc. This is because the Regge cuts have the characteristic slow logarithmic factors appearing in the amplitudes to which the cross sections may in general not be so sensitive.[4] The cuts with a suitable mechanism (like the eikonal or absorption model, which determines their weight functions in terms of the basic input parameters of the poles, would give a better test for their showing up in the polarization and density-matrix-element data[2] which are normalized with respect to the data on the differential cross section.

In this paper we have tried to analyze the data on the density-matrix elements of $A_1(1^+, 1070\text{ MeV})$ in the process $\pi p\to A_1 p$, using the 8-GeV high-energy data[5] on the differential cross section of $\pi^+ p\to A_1^+ p$. For high-energy scattering we use the Regge eikonal model in which, to the Regge-pole contributions coming from the Pomeranchukon (P) and the ρ Regge trajectories, are added the $P-P$, $P-\rho$, and $\rho-\rho$ Regge cuts. We assume here that at high energies the P couples only to the helicity-nonflip amplitude in the problem.[6]

The plan of the paper is as follows. Section II deals with some notation, kinematics, the Regge representations of the independent helicity amplitudes in the problem, and the eikonal representation of these amplitudes. In Sec. III we calculate the integrals occurring in Sec. II, and in Sec. IV we give the results of our computations and discuss and compare these with the available data.

II. FORMALISM

A. Kinematics, Notation, and Isospin Decomposition for $\pi N\to A_1 N$

We define the following kinematical variables in the s-channel scattering of

$$\pi(p_\pi, \lambda_\pi = 0) + N(p_N, \lambda_N) \to A_1(k_A, \lambda_A) + N(k_N, \lambda'_N):$$

$$s = -(p_\pi + p_N)^2,$$

$$t = -(p_\pi - k_A)^2,$$

$$u = -(p_\pi - k_N)^2.$$

The initial and final center-of-mass momenta squared are

$$q_1^{\,2} = \frac{[s-(m_\pi+m_N)^2][s-(m_N-m_\pi)^2]}{4s},$$
$$q_2^{\,2} = \frac{[s-(m_N+m_A)^2][s-(m_N-m_A)^2]}{4s}, \tag{2.1a}$$

and the center-of-mass energies are

$$E_\pi = \frac{s+m_\pi^{\,2}-m_N^{\,2}}{2\sqrt{s}},$$
$$E_A = \frac{s+m_A^{\,2}-m_N^{\,2}}{2\sqrt{s}}. \tag{2.1b}$$

The differential cross section is defined as

$$\frac{d\sigma}{dt} = \frac{2\pi s^2}{s^2 - 2s(m_N^{\,2}+m_\pi^{\,2}) + (m_N^{\,2}-m_\pi^{\,2})^2} \times \sum_{\lambda_N \lambda_A \lambda'_N} |F_{0\lambda_N, \lambda_A \lambda'_N}|^2. \tag{2.2}$$

The contributions from t-channel exchanges to $\pi^\pm p \to A_1^\pm p$ are given by

$$F^\pm(s,t) = -(1/\sqrt{6})P(s,t) \pm \tfrac{1}{2}\rho(s,t), \tag{2.3}$$

where $F^\pm(s,t)$ denote the s-channel amplitudes for the processes $\pi^\pm p \to A_1^\pm p$. In what follows, for brevity, we shall drop the superscript $\pm$. Also, here $P(s,t)$ and $\rho(s,t)$ denote the contributions to these amplitudes of the Pomeranchukon and the ρ Regge trajectories. As remarked earlier, we have assumed that the Pomeranchukon does not contribute to the spin-flip amplitudes. Lastly we define the (3×3) density matrix for the resonance $A_1(1^+)$ as

$$\rho^A_{\lambda,\mu} = N \sum_{\lambda_N \lambda'_N} F_{0\lambda_N, \lambda\lambda'_N} F^*_{0\lambda_N, \mu\lambda'_N}, \tag{2.4a}$$

where each of the two summations is carried over the helicities $\pm\frac{1}{2}$ of the initial and final protons denoted by λ_N and λ'_N, respectively. The normalization N is so chosen that

$$\mathrm{Tr}\rho_{\lambda,\mu} = 1. \tag{2.4b}$$

B. Independent Helicity Amplitudes and Their Regge Representations

The total number of helicity amplitudes in the process considered here is 12. The conservation of parity and G parity [at the $N\bar{N}\alpha$ vertex, where $\alpha(t)$ is the exchanged trajectory] allows only five independent helicity amplitudes. For definiteness, we write down the relations for our s-channel helicity amplitudes resulting from parity[7] and G-parity conservations[8] mentioned above, as follows:

$$F_{0-\lambda_N, -\lambda_A-\lambda'_N}(s,t) = \frac{\eta_A \eta_N}{\eta_\pi \eta_N}(-1)^{s_A+s_N-s_N}(-1)^{\mu-\mu'} \times F_{0\lambda_N, \lambda_A\lambda'_N}(s,t), \tag{2.5}$$

where

$$\mu = -\lambda_N, \quad \mu' = \lambda_A - \lambda'_N,$$

and

$$F_{0\lambda_N, \lambda_A\lambda'_N}(s,t) = (-1)^\lambda [gP_J(-1)^I] F_{0\lambda'_N, \lambda_A\lambda_N}(s,t), \tag{2.6a}$$

where

$$\lambda = \lambda_N - \lambda'_N.$$

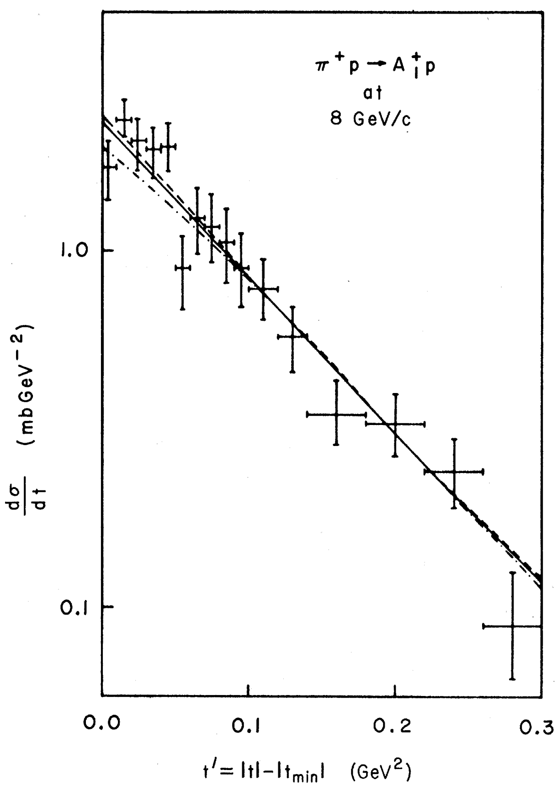

FIG. 1. Differential cross section for $\pi^+ p \to A_1^+ p$ at 8 GeV/c in the forward direction. The data are from Ref. 5. The three curves correspond to contributions from different singularities: The dashed line corresponds to the contribution from $P+\rho$ Regge trajectories, the solid line corresponds to the contribution from $P+\rho$ Regge trajectories and P-P + P-ρ Regge cuts, and the dot-dash line corresponds to the contribution from $P+\rho$ Regge trajectories and P-P + P-ρ + ρ-ρ Regge cuts.

Following the argument given in Ref. 8, we shall take the product

$$gP_J(-1)^I=+ \tag{2.6b}$$

both for the leading Regge poles and the leading Regge cuts considered here, because one assumes that the leading Regge cuts are dominated by the quantum numbers, except the parity,[9] of the leading poles. Using Eqs. (2.5), (2.6a), and (2.6b), one obtains the following five independent s-channel helicity amplitudes in our problem, which are classified according to the "magnitude" of helicity flip exchanged in the t channel. There are thus one "nonflip" amplitude,

$$F_{0\,1/2,\,0\,1/2}, \tag{2.7a}$$

three "unit-flip" amplitudes,

$$\begin{aligned}&F_{0\,1/2,\,0\,-1/2},\\&F_{0\,1/2,\,0\,1/2},\\&F_{0\,-1/2,\,1\,-1/2},\end{aligned} \tag{2.7b}$$

and one "double-flip" amplitude,

$$F_{0\,1/2,\,1\,-1/2}. \tag{2.7c}$$

At this stage, a remark is in order, which will be useful in parametrizing these amplitudes at high energies. If we were to use a definite parity at the $N\bar{N}$ vertex,[10] then the number of independent helicity amplitudes further reduces in the following manner. For natural-parity exchange, for instance, the last two of the three "unit-flip" amplitudes in Eq. (2.7b) become equal giving, thereby, four independent helicity amplitudes. For unnatural-parity exchange, however, all amplitudes vanish except again the last two of Eq. (2.7b), which are equal in magnitude but differ in phase.

The Regge behavior for these amplitudes can be derived from the general formula[10]

$$F_{\lambda_1\lambda_2,\,\lambda_3\lambda_4}(s,t)\underset{s\to\infty}{\approx}\sum_i g^{(i)}_{\lambda_1\lambda_3}(t)g^{(i)}_{\lambda_2\lambda_4}(t)\left[\left(\frac{-t}{s_0}\right)^{1/2}\right]^{|\lambda_1-\lambda_3|+|\lambda_2-\lambda_4|}\left(\frac{1\pm e^{-i\pi\alpha_i(t)}}{\sin\pi\alpha_i(t)}\right)\left(\frac{s}{s_0}\right)^{\alpha_i(t)}, \tag{2.8}$$

for the s-channel scattering $1+2\to 3+4$ of any mass particle. The sum over i denotes the sum over all possible Regge trajectories. In our problem, the P and ρ will be taken as the dominant Regge trajectories, and the rest, including the unnatural trajectories, will be ignored because of their low intercepts. Thus, on the basis of natural-parity exchange and factorization, we expect that two of the helicity "unit-flip" amplitudes for our "Born approximation" in the eikonal representation behave asymptotically in the same way, that is,

$$F_{0\,1/2,\,1\,1/2}\approx F_{0\,-1/2,\,1\,-1/2}. \tag{2.9}$$

Furthermore, for the small-momentum-transfer predictions, as usual, we shall neglect the double-flip amplitude.[11] Therefore, effectively, we shall be dealing with three independent amplitudes for our high-energy parametrization of the amplitudes taken as "input" in the eikonal representation. Using Eqs. (2.3) and (2.8) one obtains the asymptotic behavior of these amplitudes describing the processes $\pi^{\pm}p\to A_1^{\pm}p$ as

$$F^R_{0,0}(s,t)\equiv F^R_{0\,1/2,\,0\,1/2}(s,t)\approx-\frac{1}{\sqrt6}\left[-i\gamma_0^P\exp(-i\tfrac12\pi t\alpha_P')\left(\frac{s}{s_0}\right)^{\alpha_P(t)-1}\right]\pm\frac12\left[i\gamma_0^\rho\alpha_\rho(t)\exp[-i\tfrac12\pi\alpha_\rho(t)]\left(\frac{s}{s_0}\right)^{\alpha_\rho(t)-1}\right], \tag{2.10a}$$

$$F^R_{0,1}(s,t)\equiv F^R_{0\,1/2,\,0\,-1/2}(s,t)\approx\pm\frac12\left[i\left(\frac{-t}{s_0}\right)^{1/2}\gamma_1^\rho\alpha_\rho(t)\exp[-i\tfrac12\pi\alpha_\rho(t)]\left(\frac{s}{s_0}\right)^{\alpha_\rho(t)-1}\right], \tag{2.10b}$$

$$F^R_{1,0}(s,t)\equiv F^R_{0\,1/2,\,1\,1/2}(s,t)\approx F^R_{0\,-1/2,\,1\,-1/2}(s,t)\approx\pm\frac12\left[i\left(\frac{-t}{s_0}\right)^{1/2}\gamma_1'^\rho\alpha_\rho(t)\exp[-i\tfrac12\pi\alpha_\rho(t)]\left(\frac{s}{s_0}\right)^{\alpha_\rho(t)-1}\right], \tag{2.10c}$$

where γ_0^P, γ_0^ρ, γ_1^ρ, and $\gamma_1'^\rho$ are constant residue parameters for different helicity amplitudes. While writing ρ Regge amplitudes, we have assumed that the ρ trajectory satisfies the nonsense-choosing mechanism. In the above Regge representation we have ignored the rather slowly varying functions of t in the signature factors.

The trajectories are taken as

$$\begin{aligned}&\alpha_P(t)=1+t\alpha_P',\\&\alpha_\rho(t)=0.5+t\alpha',\end{aligned} \tag{2.10d}$$

with

$$\alpha_P' = 0.4, \quad \alpha' = 0.9\,.$$

Lastly, the s_0 will be fixed equal to 1 GeV^2 in our computation.

C. Eikonal Representation

We may now define the following impact-parameter representation for the various helicity amplitudes, which accounts (in addition to the P and ρ poles) for the cuts produced due to the rescattering of P with itself and with ρ, and also for the rescattering of ρ with itself. Thus, for high energy and small momentum transfer,

TABLE I. Residue parameters of fit to $\pi^+ p \to A_1^+ p$ scattering data[5]: A, taking the contributions from $P+\rho$ Regge trajectories; B, taking the contributions from $P+\rho$ Regge trajectories and P-P + P-ρ cuts; and C, taking the contributions from $P+\rho$ Regge trajectories and P-P + P-ρ + ρ-ρ cuts.

Fit	γ_0^P (GeV)	γ_0^ρ (GeV)	γ_1^ρ (GeV)	$\gamma_1'^\rho$ (GeV)
A	0.33	17.92	−5.08	−0.072
B	−0.31	−17.24	−7.10	8.03
C	0.32	17.74	−2.10	22.12

$$F_{0,0}(s,t) \approx (-i)\int_0^\infty b\,db\,J_0(b\sqrt{-t})\exp[i\chi_0(s,b^2)-1]\,, \tag{2.11a}$$

where

$$\chi_0(s,b^2) \approx \int_0^\infty \sqrt{-t}\,d\sqrt{-t}\,J_0(b\sqrt{-t})F_{0,0}^R(s,t)\,,$$

and for the two "unit-flip" amplitudes,

$$F_{0,1}(s,t) \approx \int_0^\infty b\,db\,J_1(b\sqrt{-t})\exp[i\chi_0(s,b^2)]\chi_{0,1}^R(s,b^2)\,, \tag{2.11b}$$

where

$$\chi_{0,1}^R(s,b^2) \approx \int_0^\infty \sqrt{-t}\,d\sqrt{-t}\,J_1(b\sqrt{-t})F_{0,1}^R(s,t)\,,$$

and

$$F_{1,0}(s,t) \approx \int_0^\infty b\,db\,J_1(b\sqrt{-t})\exp[i\chi_0(s,b^2)]\chi_{1,0}^R(s,b^2)\,, \tag{2.11c}$$

where

$$\chi_{1,0}^R(s,b^2) \approx \int_0^\infty \sqrt{-t}\,d\sqrt{-t}\,J_1(b\sqrt{-t})F_{1,0}^R(s,t)\,.$$

III. EVALUATION OF THE INTEGRALS AND EXPRESSIONS FOR DENSITY-MATRIX ELEMENTS

For the evaluation of the integral representations, we can simply use the formula

$$\int_0^\infty x^\mu \exp(-\alpha x^2)J_\nu(xy)\,dx = \frac{\Gamma(\frac{1}{2}\nu+\frac{1}{2}\mu+1)}{2^{\nu+1}(\sqrt{\alpha})^{\mu+\nu+1}\Gamma(\nu+1)}\,y^\nu \exp(-y^2/4\alpha)\,{}_1F_1(\tfrac{1}{2}+\tfrac{1}{2}\nu-\tfrac{1}{2}\mu,\,\nu+1;\,y^2/4\alpha)\,. \tag{3.1}$$

Thus, from Eqs. (2.10), (2.11), and (3.1), one obtains, with certain simple manipulations, the following eikonals:

$$\chi_0(s,b^2) = ir_P\left(\frac{\exp[-b^2/4\xi_P(s)]}{2\xi_P(s)}\right) + ir_\rho(s)\left(\frac{\alpha_\rho(0)\exp[-b^2/4\xi_\rho(s)]}{2\xi_\rho(s)} - \frac{\alpha'\exp[-b^2/4\xi_\rho(s)]L_1(b^2/4\xi_\rho(s))}{2[\xi_\rho(s)]^2}\right), \tag{3.2a}$$

$$\chi_{0,1}^R(s,b^2) = \tfrac{1}{4}ir_1^\rho(s)\left(\frac{\alpha_\rho(0)}{[\xi_\rho(s)]^2} - \frac{\alpha'[1+L_1(b^2/4\xi_\rho(s))]}{[\xi_\rho(s)]^3}\right)b\exp[-b^2/4\xi_\rho(s)]\,, \tag{3.2b}$$

and

$$\chi_{1,0}^R(s,b^2) = \frac{r_1'^\rho(s)}{r_1^\rho(s)}\,\chi_{0,1}^R(s,b^2)\,, \tag{3.2c}$$

where

$$r_P = \frac{1}{\sqrt{6}}\gamma_0^P(0), \qquad r_\rho(s) = \frac{1}{2}\left(\frac{s}{s_0}\right)^{-1}\gamma_0^\rho(0)\left(\exp(-i\tfrac{1}{2}\pi)\frac{s}{s_0}\right)^{\alpha_\rho(0)},$$

$$r_1^\rho(s) = \frac{1}{2\sqrt{s_0}}\left(\frac{s}{s_0}\right)^{-1}\gamma_1^\rho(0)\left(\exp(-i\tfrac{1}{2}\pi)\frac{s}{s_0}\right)^{\alpha_\rho(0)}, \tag{3.2d}$$

$$r_1'^\rho(s) = \frac{\gamma_1'^\rho(0)}{\gamma_1^\rho(0)} r_1^\rho(s), \tag{3.2e}$$

and

$$\xi_P(s)/\alpha_P' = \xi_\rho(s)/\alpha' = \ln(s/s_0) - i\tfrac{1}{2}\pi. \tag{3.2f}$$

With the eikonals given by (3.2) it is possible, in principle, to find cut effects of all orders due to the multiple Pomeranchukon exchanges. However, in the rather low momentum transfers in which we are interested, these effects may be negligible. In fact for all practical purposes the first-order cuts will be taken. Whence, reinserting these eikonals in the integral representations given by Eq. (2.11) and using Eqs. (3.2) again, one obtains

$$\begin{aligned}
F_{0,0}(s,t) \approx i\Big[&\{r_P \exp[t/4A_P(s)] + \alpha_\rho(t) r_\rho(s)\exp[t/4B_\rho(s)]\}_{\text{Pole terms}} - \{\tfrac{1}{2}r_P{}^2 A_P(s)\exp[t/8A_P(s)]\}_{P-P\ \text{cut}} \\
&- \left(\frac{2r_P r_\rho(s) A_P(s) B_\rho(s)\exp\{t/8[A_P(s)+B_\rho(s)]\}}{A_P(s)+B_\rho(s)}\;\frac{\alpha_\rho(0) - 4\alpha' B_\rho(s) + 4\alpha' B_\rho^2(s)\{1 + t/4[A_P(s)+B_\rho(s)]\}}{A_P(s)+B_\rho(s)}\right)_{P-\rho\ \text{cut}} \\
&- (\tfrac{1}{2}B_\rho(s) r_\rho{}^2(s)\exp[t/8B_\rho(s)]\{\alpha_\rho^2(0) + 16\alpha'^2 B_\rho^2(s) + 8\alpha'^2 B_\rho(s)[1 + t/8B_\rho(s) + t^2/128B_\rho^2(s)] \\
&- 4\alpha'^2 B_\rho(s)[1 + t/8B_\rho(s)] - 4\alpha'\alpha_\rho(0)B_\rho(s)[1 - t/8B_\rho(s)]\})_{\rho-\rho\ \text{cut}}\Big],
\end{aligned} \tag{3.3a}$$

$$\begin{aligned}
F_{0,1}(s,t) \approx i\sqrt{-t}\, r_1^\rho(s)\Big\{&\{\alpha_\rho(t)\exp[t/4B_\rho(s)]\}_{\rho\ \text{pole}} \\
&- \left[\left([\alpha_\rho(0) - 8\alpha' B_\rho(s)] + 8\alpha' B_\rho^2(s)\frac{1 + t/8[A_P(s)+B_\rho(s)]}{A_P(s)+B_\rho(s)}\right)\frac{2r_P A_P(s) B_\rho^2(s)\exp\{t/8[A_P(s)+B_\rho(s)]\}}{[A_P(s)+B_\rho(s)]^2}\right]_{P-\rho\ \text{cut}} \\
&- [\{r_\rho(s)\exp[t/8B_\rho(s)]\}(\tfrac{1}{2}B_\rho(s)[\alpha_\rho(0) - 4\alpha' B_\rho(s)][\alpha_\rho(0) - 8\alpha' B_\rho(s)] \\
&\qquad + 4\alpha' B_\rho^2(s)[\alpha_\rho(0) - 6\alpha' B_\rho(s)][1 + t/16B_\rho(s)] \\
&\qquad + 12\alpha'^2 B_\rho^3(s)\{1 + t/8B_\rho(s) + [t/8B_\rho(s)]^2/6\})]_{\rho-\rho\ \text{cut}}\Big\},
\end{aligned} \tag{3.3b}$$

and

$$F_{1,0}(s,t) \approx \frac{r_1'^\rho(s)}{r_1^\rho(s)} F_{0,1}(s,t), \tag{3.3c}$$

TABLE II. Values of ρ_{00} and Reρ_{10} including $P+\rho$ contributions to $\pi^-p \to A_1^-p$. Experimental values are from Ref. 12. (a) At low energy which is the sum of 5-, 7-, and 7.5-GeV/c data. (b) At high energy which is the sum of the 11-, 13-, 20-, and 25-GeV/c data.

ρ	$\lvert t\rvert - \lvert t_{\min}\rvert$ (GeV^2)	Theoretical values [a] at 5 GeV/c	at 8 GeV/c	at 16 GeV/c	at 25 GeV/c	Experimental values (a)	(b)
ρ_{00}	0.0–0.1	1.00–1.00	1.00–1.00	1.00–1.00	1.00–1.00	0.89 ± 0.02	0.94 ± 0.05
	0.1–0.2	1.00–1.00	1.00–1.00	1.00–1.00	1.00–1.00	0.74 ± 0.03	0.77 ± 0.08
	0.2–0.4	1.00–1.00	1.00–1.00	1.00–1.00	1.00–1.00	0.41 ± 0.06	0.46 ± 0.13
Reρ_{10}	0.0–0.1	−0.00–−0.00	−0.00–−0.00	−0.00–−0.00	−0.00–−0.00	0.16 ± 0.01	0.15 ± 0.02
	0.1–0.2	−0.00–−0.00	−0.00–−0.00	−0.00–−0.00	−0.00–+0.00	0.28 ± 0.02	0.28 ± 0.05
	0.2–0.4	−0.00–+0.00	−0.00–+0.00	−0.00–+0.00	+0.00–−0.00	0.31 ± 0.04	0.35 ± 0.08

[a] The first (second) column of the theoretical values corresponds to the first (second) columns for $\lvert t\rvert - \lvert t_{\min}\rvert$.

where

$$A_P(s)=\frac{1}{4\xi_P(s)} \quad\text{and}\quad B_\rho(s)=\frac{1}{4\xi_\rho(s)}, \tag{3.3d}$$

with ξ_P and ξ_ρ defined by (3.2f).

To conclude this section we give the expressions for the density-matrix elements which are to be calculated using the amplitude given by (3.3). From the general formula (2.4a), the density-matrix elements ρ_{00} and $\mathrm{Re}\rho_{10}$ may be derived immediately as

$$\rho_{00}=\frac{|F_{0\,1/2,0\,1/2}|^2+|F_{0\,1/2,0\,-1/2}|^2}{|F_{0\,1/2,0\,1/2}|^2+F_{0\,1/2,0\,-1/2}|^2+2|F_{0\,1/2,1\,1/2}|^2},$$

$$\mathrm{Re}\rho_{10}=\frac{\mathrm{Re}F_{0\,1/2,1\,1/2}\,\mathrm{Re}F_{0\,1/2,0\,1/2}+\mathrm{Im}F_{0\,1/2,1\,1/2}\,\mathrm{Im}F_{0\,1/2,0\,1/2}}{|F_{0\,1/2,0\,1/2}|^2+|F_{0\,1/2,0\,-1/2}|^2+2|F_{0\,1/2,1\,1/2}|^2}, \tag{3.3e}$$

where we have neglected the contribution of the "double-flip" amplitude to the differential cross section.

IV. RESULTS AND DISCUSSION

We have used seven data points (for $|t|=0.08$–$0.24\ \mathrm{GeV}^2$) at the 8-GeV/c measurements of the $\pi^+p\to A_1^+p$ differential cross section[5] for determining the four parameters γ_0^P, γ_0^ρ, γ_1^ρ, and $\gamma_1'^\rho$ in our work. Three sets of these parameters have been determined from a fit to the above cross-section data for three different cases A, B, and C depending on the choice of t-channel singularities. For case A of the fit we take the P and ρ trajectories, for case B the P-P and the P-ρ cuts are added to case A Regge-pole terms, and, finally, for case C the ρ-ρ cut contributions are also added to the previous singularities. The values of the parameters from these fits are listed in Table I. Using these parameters we find that in all cases the theoretical values for the differential cross section are in good agreement with the experiment only up to $|t|=0.8\ \mathrm{GeV}^2$. The above parameters are also used to determine the density-matrix elements ρ_{00} and $\mathrm{Re}\rho_{10}$ for A_1^- in the process $\pi^-p\to A_1^-p$ at several high energies for the cases of three different t-channel singularity exchanges defined above. Table II compares the theoretical values of ρ_{00} and $\mathrm{Re}\rho_{10}$ with the corresponding experimental values. The theoretical numbers in case A for ρ_{00} are nearly 1.0 and those for $\mathrm{Re}\rho_{10}$ are nearly zero for the small momentum transfer range considered. Evidently they are in total disagreement with the experimental numbers[12] because the Pomeranchukon trajectory points to the s-channel helicity conservation, whereas experimentally this is not satisfied in the $\pi^-p\to A_1^-p$ process. Similar results are obtained if we take contributions only from the ρ trajectory. The inclusion of the P-P and the P-ρ cut contributions to the density-matrix elements, as can be seen from Table III, does not much improve the predictions. Table IV supplies the density-matrix elements for case C where the ρ-ρ cut is included in addition to the poles and the remaining two cuts. The agreement here is reasonably good. For the momentum transfer range of $|t|-|t_{\min}|$ up to 0.3 GeV^2, the predicted numbers for both ρ_{00} and $\mathrm{Re}\rho_{10}$ are in agreement. At $|t|-|t_{\min}|=0.4\ \mathrm{GeV}^2$, the theoretical value for

TABLE III. Values of ρ_{00} and $\mathrm{Re}\rho_{10}$ for $\pi^-p\to A_1^-p$ taking $P+\rho$ Regge trajectories, P-P +P-ρ cuts. Experimental values are the same as those used in Table II.

ρ	$\lvert t\rvert-\lvert t_{\min}\rvert$ (GeV^2)	Theoretical values[a] at 5 GeV/c	at 8 GeV/c	at 16 GeV/c	at 25 GeV/c	Experimental values (a)	(b)
ρ_{00}	0.0–0.1	1.00–0.94	1.00–0.93	1.00–0.92	1.00–0.91	0.89±0.02	0.94±0.05
	0.1–0.2	0.94–0.85	0.93–0.83	0.92–0.86	0.91–0.91	0.74±0.03	0.77±0.08
	0.2–0.4	0.85–0.98	0.83–0.99	0.86–1.00	0.91–1.00	0.41±0.06	0.46±0.13
$\mathrm{Re}\rho_{10}$	0.0–0.1	0.00– –0.16	0.00– –0.16	0.00– –0.16	0.00– –0.13	0.16±0.01	0.15±0.02
	0.1–0.2	–0.16– –0.21	–0.16– –0.17	–0.16– –0.04	–0.13– –0.04	0.28±0.02	0.28±0.05
	0.2–0.4	–0.21–0.07	–0.17–+0.05	–0.04–+0.03	–0.04–+0.02	0.31±0.04	0.35±0.08

[a] The first (second) column of the theoretical values corresponds to the first (second) columns for $|t|-|t_{\min}|$.

TABLE IV. Values of ρ_{00} and Reρ_{10} for $\pi^- p \to A_1^- p$ taking $P+\rho$ Regge trajectories, P-P +P-ρ +ρ-ρ cuts. Experimental values are the same as those used in Table II.

ρ	$\lvert t\rvert - \lvert t_{min}\rvert$ (GeV^2)	Theoretical values at 5 GeV/c	at 8 GeV/c	at 16 GeV/c	at 25 GeV/c	Experimental values (a)	(b)
ρ_{00}	0.0	1.00	1.00	1.00	1.00		
	0.04	0.87	0.86	0.83	0.81		
	0.08	0.76	0.72	0.67	0.65	0.89 ± 0.02	0.94 ± 0.05
	0.10	0.70	0.66	0.65	0.58		
	0.12	0.65	0.60	0.54	0.53		
	0.16	0.54	0.48	0.44	0.48	0.74 ± 0.03	0.77 ± 0.08
	0.20	0.42	0.37	0.41	0.55		
	0.24	0.31	0.31	0.51	0.69		
	0.28	0.25	0.38	0.68	0.83		
	0.30	0.28	0.48	0.77	0.88	0.41 ± 0.06	0.46 ± 0.13
	0.35	0.57	0.58	0.87	0.93		
	0.40	0.87	0.93	0.97	0.99		
Reρ_{10}	0.0	0.10	0.10	0.10	0.10		
	0.04	0.23	0.24	0.25	0.24		
	0.08	0.30	0.30	0.29	0.26	0.16 ± 0.01	0.15 ± 0.02
	0.10	0.31	0.32	0.29	0.24		
	0.12	0.32	0.32	0.28	0.20		
	0.16	0.33	0.31	0.20	0.08	0.28 ± 0.02	0.28 ± 0.05
	0.20	0.31	0.25	0.06	−0.07		
	0.24	0.24	0.12	−0.10	−0.16		
	0.28	0.10	−0.07	−0.19	−0.18		
	0.30	−0.00	−0.15	−0.20	−0.17	0.31 ± 0.04	0.35 ± 0.08
	0.35	−0.11	−0.15	−0.14	−0.10		
	0.40	−0.20	−0.15	−0.09	−0.07		

ρ_{00} is rather large and in that range Reρ_{10} becomes negative. This may be due to the fact that the data employed for our parameter is determined from the $\pi^+ p \to A_1^+ p$ process, whereas we are determining the density-matrix elements of A_1^- in the crossed process of $\pi^- p \to A_1^- p$. Furthermore, for large momentum transfers, higher-order cuts ignored here may have an important effect. We have also compared the density-matrix elements ρ_{00} and Reρ_{10} for A_1^+ in $\pi^+ p \to A_1^+ p$ by taking contributions from $P+\rho$ poles and P-P, P-ρ, and ρ-ρ cuts given in Table V. Again it is obvious from this table that our values are consistent with the experimental values[13] only in the $\lvert t\rvert = 0.0$–0.3 GeV^2 region.

To conclude we may remark that the ρ-ρ-cut

TABLE V. Values of ρ_{00} and Reρ_{10} including $P+\rho$ Regge trajectories and P-P +P-ρ +ρ-ρ cuts to $\pi^+ p \to A_1^+ p$. Experimental values are from Ref. 13.

ρ	$\lvert t\rvert - \lvert t_{min}\rvert$ (GeV^2)	Theoretical values at 5 GeV/c	at 8 GeV/c	at 16 GeV/c	at 25 GeV/c	Experimental values at 8 GeV/c	at 16 GeV/c
ρ_{00}	0.0	0.97	0.97	0.98	0.98		
	0.1	0.80	0.83	0.87	0.89	1.10 ± 0.05	0.84 ± 0.05
	0.2	0.75	0.79	0.86	0.89	0.65 ± 0.08	0.65 ± 0.06
	0.3	0.81	0.84	0.92	0.95	0.56 ± 0.12	0.23 ± 0.13
	0.4	0.94	0.86	0.98	0.99		
Reρ_{10}	0.0	0.08	0.07	0.04	0.02		
	0.1	0.28	0.26	0.23	0.21	0.15 ± 0.04	0.20 ± 0.04
	0.2	0.30	0.28	0.23	0.20	0.27 ± 0.04	0.32 ± 0.04
	0.3	0.26	0.24	0.17	0.14	0.30 ± 0.07	0.35 ± 0.65
	0.4	0.16	0.23	0.8	0.06		

contribution plays an important role in the process, although this cut may not be realistic, because the eikonal model does not give any idea about the quantum numbers and signature correctly and a few workers[14] are also in doubt about the validity of Regge-Regge cuts in the eikonal prescription.

ACKNOWLEDGMENTS

The authors are grateful to Dr. B. K. Agarwal, Dr. M. S. K. Razmi, Dr. M. M. Islam, Dr. G. Alberi, and Dr. M. Barmawi for fruitful discussions. They would also like to thank Professor Abdus Salam and Professor P. Budini, the International Atomic Energy Agency, and UNESCO for hospitality at the International Centre for Theoretical Physics, Trieste. One of us (M.B.B.) is greatly indebted to Dr. M. Taslimi, Chancellor, Tabriz University, Iran, for his financial support.

---

[1]S. C. Frautschi and F. Ravndal, Caltech Report No. CALT-68-268, 1970 (unpublished), and references therein for earlier works; also F. Henyey, G. L. Kane, J. Pumplin, and M. H. Ross, Phys. Rev. 182, 1579 (1969).

[2]M. Colocci, Lett. Nuovo Cimento 4, 53 (1970); A. P. Contogouris, J. P. Lebrun, and G. von Bochman, Nucl. Phys. B13, 246 (1969); A. Sundaram, Lett. Nuovo Cimento 1, 177 (1971).

[3]S. Mandelstam, Nuovo Cimento 30, 1127 (1963); D. Amati, S. Fubini, and A. Stanghellini, *ibid.* 26, 896 (1962); V. N. Gribov, I. Ya. Pomeranchuk, and K. A. Ter-Martirosyan, Phys. Rev. 139, B814 (1965).

[4]Pole-plus-cut models, however, in some cases, may give important interference effects in cross sections. See for instance Refs. 1 and 2.

[5]M. Aderholz *et al.*, Nucl. Phys. B8, 45 (1968).

[6]R. C. Arnold, Phys. Rev. 153, 1523 (1967).

[7]We adopt the same convention for our helicity amplitudes as that of M. Jacob and G. C. Wick, Ann. Phys. (N.Y.) 7, 404 (1959), except that we do not include the over-all phase factors (see Ref. 10) for these amplitudes.

[8]A. B. Kaidalov, Phys. Letters 26B, 20 (1967).

[9]V. N. Gribov, in *Proceedings of the Twelfth International Conference on High Energy Physics, Dubna, 1964* (Atomizdat, Moscow, U.S.S.R., 1966), p. 394; Yadern. Fiz. 5, 197 (1967) [Soviet J. Nucl. Phys. 5, 138 (1967)].

[10]G. Cohen-Tannoudji, Ph. Salin, and A. Morel, Nuovo Cimento 55A, 412 (1968).

[11]Because of the factor $(\sqrt{-t})^n$ in Eq. (2.8), where n is the total spin flip in the t channel, the magnitude of the double-flip amplitude in the region of small momentum transfer will be much smaller than the other amplitudes.

[12]G. Ascoli *et al.*, Phys. Rev. Letters 26, 929 (1971).

[13]Aachen-Berlin-Bonn-CERN-Cracow-Heidelberg-London-Vienna Collaboration, Phys. Letters 34B, 161 (1971).

[14]J. Finkelstein, Nuovo Cimento 5A, 413 (1971), and references therein.